

FEA Model and Mechanical Analysis of the Nb₃Sn 15 T Dipole Demonstrator

C. Kokkinos, I. Apostolidis, J. Carmichael, T. Gortsas, S. Kokkinos, K. Loukas, I. Novitski, D. Polyzos, D. Rodopoulos, D. Schoerling, D. Tommasini, A.V. Zlobin

Abstract— Nb₃Sn magnets with a nominal operation field of ~15 T are being considered for the LHC energy upgrade (HE-LHC) and a post-LHC Future Circular Collider (FCC). To demonstrate the feasibility of 15 T accelerator quality dipole magnets, the US Magnet Development Program (MDP) is developing a single-aperture 15 T Nb₃Sn dipole demonstrator based on a 4-layer graded cos-theta coil with 60 mm aperture and cold iron yoke. The main design challenges for 15 T accelerator magnets include large Lorentz forces at this field level. To counteract them, an innovative mechanical structure based on a vertically split iron yoke, locked by large aluminum IC-clamps and supported by a thick stainless steel skin, has been developed at Fermilab. To study the performance of the structure a parametric multi-physics FEA model has been set-up. This paper describes the numerical model as well as the results of a sensitivity analysis of the effect of geometrical tolerances and assembly parameters.

Index Terms—Accelerator magnets, Design Engineering, Finite Element Analysis, Niobium-Tin, Superconducting materials

I. INTRODUCTION

THE FCC is a future Hadron Collider (HC) which will most likely succeed the LHC as the most powerful particle accelerator, providing scientists with a discovery tool in the field of high energy physics. It will be constructed in a tunnel of ~100 km in length and will require dipole magnets with a nominal operation field of ~15 T and ~20% margin. Nb₃Sn is the most likely option for the conductor technology, which sets stringent requirements for the coil fabrication technology and the mechanical structure of the magnet cold mass. The development of a 15 T magnet implies a number of challenges such as a considerably larger coil volume, higher Lorentz forces and larger stored energy in comparison to the present accelerator magnets. For the realization of an accelerator of this magnitude, it is essential to demonstrate that magnets can indeed produce such a magnetic field whilst respecting the accelerator requirements.

The US Magnet Development Program [1] is developing a single-aperture 15 T Nb₃Sn dipole demonstrator [2] based on a

This work was supported by Fermi Research Alliance, LLC, under contract No. DE-AC02-07CH11359 with the U.S. Department of Energy.

C. Kokkinos, I. Apostolidis, S. Kokkinos and K. Loukas are with FEAC Engineering P.C., 26442 Patras, Greece (phone +30 2613 019794; e-mail: charilaos.kokkinos@feacomp.com).

J. Carmichael, I. Novitski, A.V. Zlobin are with Fermi National Accelerator Laboratory, Batavia, IL 80510 USA.

D. Schoerling and D. Tommasini are with CERN (European Organization for Nuclear Research), CH 1211 Geneva, Switzerland.

T. Gortsas, D. Polyzos and D. Rodopoulos are with UPATRAS (University of Patras), 26504 Rio Achaia, Greece.

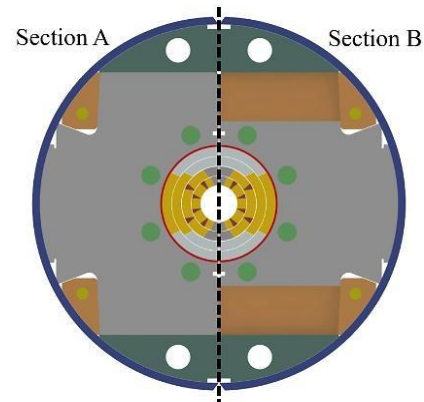


Fig. 1. Cross section of the 15 T Nb₃Sn dipole magnet.

4-layer graded cos-theta coil [2], [3] with 60 mm aperture and cold iron yoke (Fig. 1). An innovative mechanical structure to counteract the high magnetic forces, has been developed by FNAL, serving as the baseline design [4], [5]. FEAC Engineering, in collaboration with CERN, FNAL and UPATRAS continued the engineering simulation work, in terms of Finite Element (FE) and Boundary Element (BE) Analysis. The new model implements the latest modifications in the baseline design, which include the use of the IC-clamps instead of the C- and I-clamps [4], a welded skin instead of a bolted skin and updated material properties of the coil. In view of the first mechanical model assembly and test, and later on with the first model test, the effect of the material, manufacturing and assembly parameters need to be understood and any design limitations to be addressed.

This paper presents the updated design, the optimized assembly parameters and the sensitivity analysis of them on the design space of the structure.

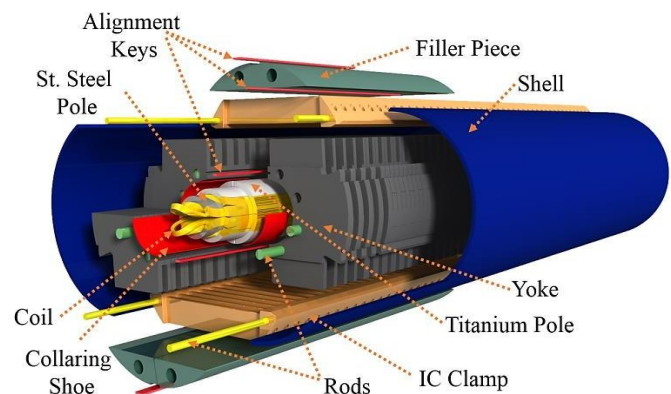


Fig. 2. Exploded view of the 15 T Dipole showing the main design features.

II. MECHANICAL STRUCTURE

A. Main design features

The main features of the 15 T design are illustrated in Figure 2. The Nb₃Sn coils are epoxy impregnated with four winding layers. The coil is based on the optimized cos-theta design with a 60 mm aperture. The chosen coil aperture is convenient for reusing the 11 T dipole coil tooling [6] and also provides enough space for a beam screen to intercept the large synchrotron radiation expected in a 100 TeV scale HC. The two innermost layers (layer 1 and 2) are comprised of five blocks separated by three wedges, while the two outermost layers (layer 3 and 4) do not use wedges. Titanium poles are impregnated with layer 1 and 2 of the coil, while layer 3 and 4 are impregnated with st. steel poles (Fig. 3) [5].

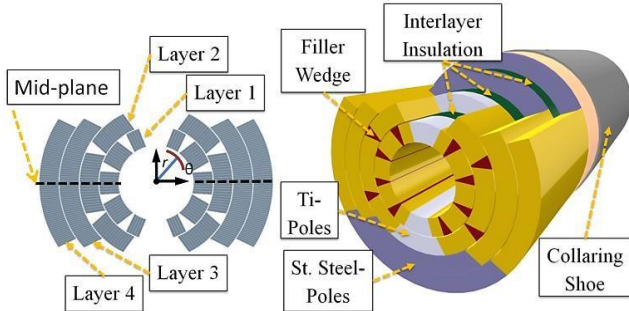


Fig. 3. 15T Dipole coil cross section [3] and key features. Both double-layer coils are impregnated with the poles. The inner coil is also impregnated with the wedges. The cylindrical coordinates, namely the radial (r) and the azimuthal (θ), are shown.

To build a more cost-effective magnet, a collarless design is adopted. This design places a 2-mm thick steel collaring shoe between the coil and yoke (Fig. 3) which protects the coil from immediate contact with the yoke. The iron laminated yoke, with an outer diameter of 587 mm, is made in two halves with a vertical split. The split is straight with an offset of 0.5 mm from the vertical plane (Fig.4), such that when the magnet is assembled and pre-stressed at room temperature, the half yokes are not in contact. On the contrary, at cryogenic temperature and during powering the gap closes firmly. This provides some elasticity to the yoke to store strain energy against the enormous Lorentz forces from the coils and creates a very rigid structure to sustain the magnetic forces and to avoid coil deformation that could affect the quench performance and field quality.

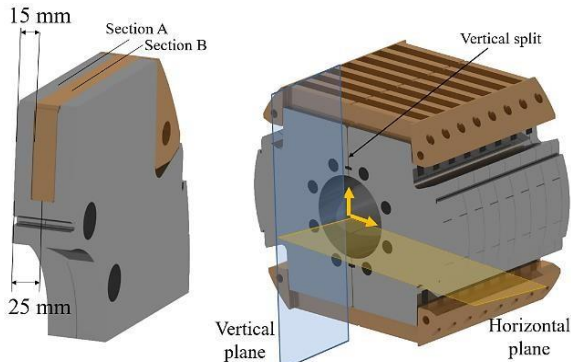


Fig. 4. The IC-clamps interleave with the iron yoke laminations.

Aluminum IC-clamps interleave with the yoke laminations so as to constrain and provide rigidity to the structure (Fig. 1, Fig.4). The IC-clamps interleave with the iron yoke laminations at their top and bottom sectors, thus reducing the iron filling factor in these areas to ~60%. The 25-mm-thick yoke laminations have a cutout to house the IC-clamps. The thickness at the interface between two yoke laminations is 25 mm, whereas at the interface between the laminations and the IC-clamps the thickness is 15 mm (Fig.4).

A steel filler piece is used to fill the space above the yoke and the IC-clamps completing the cylindrical shape of the dipole. The 12-mm-thick st. steel outer shell is made in two halves and welded at the vertical plane. The welded shell encompasses the whole structure and the weld shrinkage provides pre-stress to the assembly at room temperature.

B. Shim locations

The baseline design, with the use of the IC-clamps, allows the tailoring of the coil pre-compression to counter-balance the effects of the electromagnetic forces and to minimize the stress gradients across the brittle Nb₃Sn coils. The shim locations considered in this study are shown in Figure 5.

The inner mid-plane shim (1) which extends over layer 1 and 2 of the coil, and the outer mid-plane shim (2) which

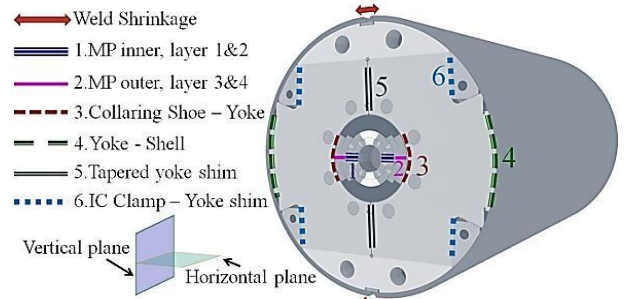


Fig. 5. Most important shim locations in the 15 T dipole.

extends over layer 3 and 4 (2) are primarily used for the adjustment of the azimuthal pre-stress in the coil. The radial shim between the collaring shoe and the yoke (3) can be used to compensate for the tendency of the coil to become oval along the horizontal axis during powering, by pushing towards the center. The same principle is considered for the use of the radial shim at the yoke-shell interface (4). The tapered shim (5) ensures that during cool-down and powering the yoke gap closes firmly and maximizes the contact area between the two half yokes. The shim at the IC-clamp - yoke interface (6) further assists to keep the gap between the half yokes closed during cool-down and powering.

III. DESIGN GOALS

The design goals of the 15 T dipole are summarized below:

1. The coils shall be solidly clamped to minimize any dimensional distortions and conductor movements. The maximum value for the acceptable coil stress is still a subject of debate in the magnet community, but keeping it about

170 MPa at the nominal design field of 15 T, and below 200 MPa at higher fields is generally considered acceptable in this study.

2. Based on the current technology utilized at FNAL, the poles are impregnated with the coil. Though, in order to understand the behavior of the coil in this interface and to possibly study the pole-loading concept [4] on this design, the pole regions are not assumed to be glued. The potential unloading of the coil shall be minimized.

3. At room temperature the yoke gap shall remain open while at cryogenic temperature and during excitation, it shall remain firmly closed at least up to the nominal design field of 15 T.

4. Weld shrinkage of up to 1mm can be obtained with present welding techniques and the stainless steel outer shell tension shall be kept below 320 MPa at the ambient temperature. Peak stresses are expected to occur locally at the welding area.

5. The behavior of the magnet structure shall be simulated up to 17 T as well, to provide insight about the performance and limits of the structure.

IV. NUMERICAL MODEL

A. Electromagnetic analysis

The electromagnetic model is analyzed in Maxwell [7] and PITHIA [8], [9] to compare results between the finite element (FEM) and boundary element method (BEM).

A non-linear B-H curve is used to describe the magnetization of the yoke. In PITHIA only the boundaries of the model are meshed and internal points are added where the results are computed. In MAXWELL, the mesh consists of triangular elements, generated by an adaptive analysis until the energy error is less than the target of 0.01 %. The 2D magnetic field distribution at 15 T is shown in Figure 6. The electromagnetic forces computed in MAXWELL were mapped onto the structural mesh.

TABLE I
15 T DIPOLE MAGNETIC RESULTS

Bo (T)	PITHIA		Maxwell	
	I (kA)	I (kA)	Fx (MN/m)	Fy (MN/m)
15	10.32	10.35	6.35	-3.65
16	11.09	11.13	7.17	-4.21
17	11.86	11.92	8.05	-4.82

B. Structural Analysis

The multi-physics model is solved in the integrated design environment of ANSYS® [7] and SIEMENS PLM Simcenter 3D® [10]. The model utilizes the plane stress boundary normal and includes a friction coefficient of 0.2 at all contact

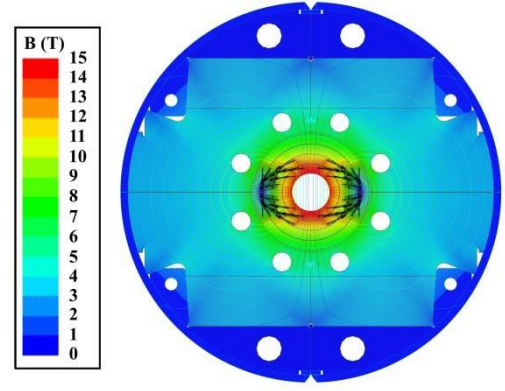


Fig. 6. Magnetic analysis of the dipole magnet at 10.32 kA, 15 T. The Lorentz forces are shown in black arrows.

interfaces. The two coils are modeled as two multi-body parts each one representing the inner and outer coil. The multi-body parts share common nodes at the interfaces of the bodies without the need of contact definitions, so as to represent the impregnation. The mesh is comprised mainly by quad elements with an orthogonal quality of 0.989. The yoke lamination and the IC-clamps are modeled as two overlapping layers. All parts have a thickness of 1mm except for the yoke lamination and the IC-clamps, which are defined at 0.6 mm and 0.4 mm, depending on the section (Fig.4). All parts are modeled with isotropic properties except for the coil which is modeled with anisotropic material properties (Table II, nominal values). The nodal coordinate system of the coil is set to a cylindrical one (Fig. 3) to account for the correct definition of the anisotropic material properties.

Five load-steps (LS) were considered in the FEM:

LS1: Yoke assembly at 293 K.

LS2: At 4.2 K.

LS3: At 4.2 K, 15 T

LS4: At 4.2 K, 16 T

LS5: At 4.2 K, 17 T

The design study converged to the shim thicknesses listed in Table II (nominal values), to meet the design goals at all times.

The Von-Mises stress evolution in the coil is presented in Fig. 7. During the welding of the shell, the peak stress is 119 MPa located on the mid-plane of layer 3. After cool-down the contraction of the cold mass structure increases the coil

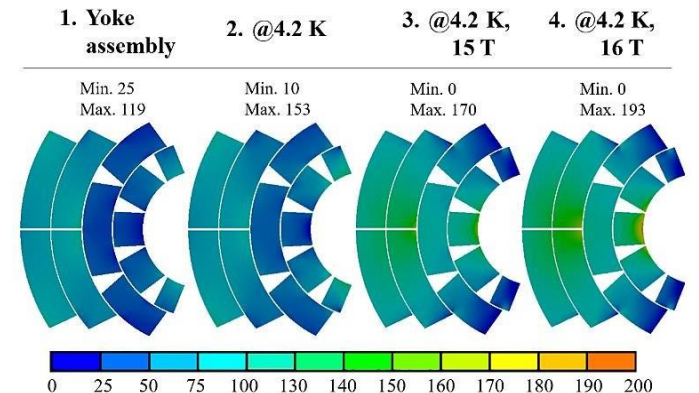


Fig. 7. Von-Mises stress (MPa) evolution in the coil. The peak stress remains below 200 MPa up to 16 T.

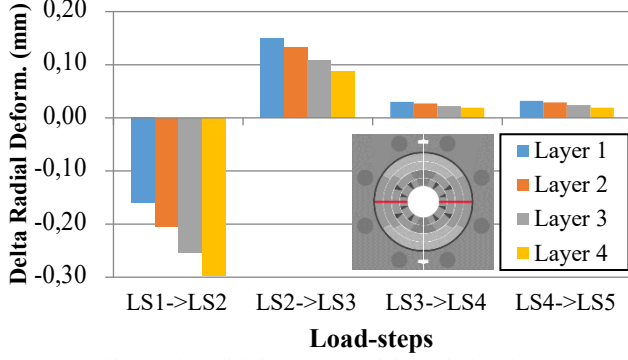


Fig. 8. Difference in radial deformation of the mid-plane between two sequential load-steps of layer 1, 2, 3 and 4.

stress by 34 MPa, this time the peak stress being located at the innermost layer, at the upper wedge - coil interface. The powering of the magnet at 15 T and the resulting Lorentz Forces increase the coil compression by 17 MPa, peaking at 170 MPa in the same location as in LS1. At 16 T, the peak stress of 193 MPa is observed in the mid-plane of layer 1. At 17 T, the peak stress increases by about 30 MPa, reaching 224 MPa and is located once again at the mid-plane of layer 1. Layer 2 of the coil is consistently the least loaded layer, while layer 1 exhibits the maximum stresses at all load-steps with the exception of LS1.

The maximum Von-Mises stress at the yoke is 261 MPa after shell welding, while at cryogenic temperature it ranges between 320 (LS2) - 350 MPa (LS5).

After the welding process, the peak azimuthal stress value of 582 MPa at the shell is localized in the welding area. By excluding the welding area, the maximum stress at ambient temperature is 316 MPa while at cryogenic temperature the peak stress ranges between 365 (LS2) - 370 MPa (LS5).

The maximum equivalent stress at the filler piece ranges between 118 MPa (LS1) and 141 MPa (LS5).

After shell welding the yoke gap is open while after cool down it remains closed at all times. The contact pressure is 85 MPa, 52 MPa, 54 MPa and 64 MPa for the load-steps LS2, LS3, LS4 and LS5 respectively.

Figure 8 presents the differential radial deformation of the coil layers at the mid-plane, between two sequential load-steps. The deformation of layer 4 reflects the behavior of the yoke at its mid-plane, as there is firm contact between the outer layer of the coil, the collaring shoe, the radial shim and the yoke. The influence of the elasticity of the coil can be seen, on the mid-plane of layer 1, 2 and 3. During excitation, layer 1 pushes against the soft material of the coil on layer 2, 3 and 4, thus allowing for larger displacement than layer 4 which pushes against the rigid envelope formed by the yoke.

C. Design Space and Sensitivity Analysis

The sensitivity analysis is conducted by utilizing the DoE method (Design of Experiments) which determines sampling points used to construct a response surface. Eleven geometric and material input parameters (Table II) were chosen for this

TABLE II
MATERIAL PROPERTIES AND SHIMS TOLERANCES FOR DOE

Property	Nominal Value	Tolerance
$E_{r,coil}$	44 GPa @ 293 K 55 GPa @ 4.2 K	20 – 60 GPa 25 – 77 GPa
$E_{\theta,coil}$	44 GPa @ 293 K 44 GPa @ 4.2 K	20 – 60 GPa 20 – 60 GPa
$a_{r,coil}$	2.6 mm/m	2 – 3 mm/m
$a_{\theta,coil}$	3.5 mm/m	3 – 4 mm/m
Weld Shrinkage (per half shell)	0.4 mm	0.35 – 0.45 mm
MP Inner (shim 1)	0 mm	0 – 0.06 mm
MP Outer (shim 2)	0.06 mm	0 – 0.09 mm
Col. Shoe – Yoke (shim 3)	0.025 mm	0 – 0.06 mm
Yoke – Shell (shim 4)	0.6 mm	0.55 – 0.65 mm
Yoke - Yoke (shim 5)	0.36 mm (avg.)	0.31 – 0.41 mm
IC clamp - Yoke (shim 6)	0.4 mm	0.35 – 0.45 mm

study, corresponding to 206 sampling points with the CCD (Central Composite Design) algorithm. The produced response surface is a full 2nd-order polynomial. The shims presented in Figure 5 are used both to apply pre-compression to the coil but also to account for geometrical instabilities of several parts due to fabrication imperfections. Thus, the manufacturing tolerances are taken into account by means of shims, e.g. the mid-plane shims (1, 2 of Fig. 5) can counterbalance any distortions in the azimuthal length of the coils. The material properties of the coil are still a subject of discussion in the

TABLE III
SENSITIVITY ANALYSIS RESULTS

Parameter	Coil Von-Mises @ 293 K (nominal : 119 MPa)		Coil Von-Mises @ 4.2 K (nominal: 153 MPa)	
	Range (MPa)	$\Delta\sigma_{max}$ (MPa)	Range (MPa)	$\Delta\sigma_{max}$ (MPa)
Weld Shrinkage	117-120	3	152-154	2
MP Inner (1)	109-119	10	153-179	26
MP Outer (2)	102-145	43	151-162	11
Col. Shoe - Yoke (3)	119-138	19	143-178	35
Yoke - Shell (4)	118-120	2	152-154	2
Yoke - Yoke (5)	103-120	17	128-178	50
IC clamp – Yoke (6)	113-123	10	152-155	3
$E_{r,coil}$	118-124	6	153-154	1
$E_{\theta,coil}$	100-141	41	97-177	80
$a_{r,coil}$	119-119	0	126-216	90
$a_{\theta,coil}$	119-119	0	143-163	20
Parameter	Coil Von-Mises @ 15 T (nominal: 170 MPa)		Coil Von-Mises @ 16 T (nominal: 193MPa)	
	Range (MPa)	$\Delta\sigma_{max}$ (MPa)	Range (MPa)	$\Delta\sigma_{max}$ (MPa)
Weld Shrinkage	170-171	1	192-194	2
MP Inner (1)	170-218	48	193-241	48
MP Outer (2)	170-196	26	192-205	13
Col. Shoe - Yoke (3)	170-180	10	183-205	22
Yoke - Shell (4)	170-171	1	192-194	2
Yoke - Yoke (5)	167-177	10	189-199	10
IC clamp - Yoke (6)	170-171	1	191-195	4
$E_{r,coil}$	170-187	17	188-214	26
$E_{\theta,coil}$	136-199	63	157-226	69
$a_{r,coil}$	168-213	45	193-234	41
$a_{\theta,coil}$	164-177	13	190-198	8

community. The tolerances have a wide range, leading to a response surface that covers a large design space.

Table III presents the effect of the design parameters on the Von-Mises stress of the coil at all load-steps, according to the tolerances described in Table II. During LS1 (yoke assembly) the outer mid-plane shim and the collaring shoe-yoke shim have the largest impact on the coil stress. The mid-plane shim exerts pressure on the coil in the azimuthal direction and the coil-yoke shim in the radial direction. The thicker the shims are, the more pressure is exerted on the coil. For the tapered shim at the yoke-yoke interface there is a limit imposed on its thickness due to the specification that the yoke gap shall remain open at room temperature. A thick shim reduces the coil stress but closes the gap. The azimuthal elastic modulus $E_{\theta,coil}$, is the material property that has the largest impact on the coil stress at this step. As the structure is shimmed, the coil is deformed elliptically along the vertical plane. Because of this deformation and the pressure exerted by the outer mid-plane shim on the coil in the azimuthal direction, variations of $E_{\theta,coil}$ have greater impact at this step than those of the radial elastic modulus $E_{r,coil}$.

During LS2 (cool down) the shims with the greatest impact on the coil stress are the tapered yoke shim and the collaring shoe - yoke shim. At cryogenic temperatures, the yoke gap is closed and the yoke becomes a rigid envelop around the coil. The maximum equivalent stress in the coil moves from layer 3 at LS1 to layer 1 (Fig. 7). The impact of the outer mid-plane shim is diminished and the inner mid-plane shim has greater effect on the coil stress. The effect of the coefficients of thermal expansion becomes apparent. The high impact of the radial thermal expansion coefficient $a_{r,coil}$, reveals the shrinkage of the coil mainly along the radial direction. As $a_{r,coil}$ increases, the coil contracts more and the pressure exerted on it from the rest of the structure lessens. Thus, the stress in the coil is decreased. The azimuthal elastic modulus $E_{\theta,coil}$ maintains a decreased, comparing to LS1, but still high impact on the coil stress as the elliptical deformation of the coil lessens, restoring part of its circular shape.

During powering, at LS3 and LS4, the Lorentz forces tend to unload the pole-turns of the coil from the pole and to deform it towards the mid-plane (Fig. 6). At the same time, the

envelope created by the two half yokes which are in contact, allows the coil to deform mainly along its length. Consequently, the coil is unloading from the poles and deforms mainly azimuthally. Therefore, the azimuthal elastic modulus $E_{\theta,coil}$ has the most significant impact on the coil stress.

At LS3 and LS4, the maximum coil stress returns to the mid-plane of layer 1 while an area of high stress appears on layer 3 (Fig. 7). The mid-plane shims, mainly the inner, have a large effect on the coil stress as well. The importance of the radial thermal expansion coefficient $a_{r,coil}$, remains high, since the structure is at a cryogenic temperature.

All rest shims and material properties have much lower effect on the coil stress in the range of variation that was imposed on them.

V. CONCLUSION

The latest modifications in the baseline design of the 15 T dipole demonstrator and the computed results from the fully parametric multi-physics FE analysis confirm the magnet support structure and its ability to manage the large level of Lorentz forces. This design reveals that coil pre-stress can be applied in a well-controlled manner and that the structure allows keeping the stress in the coil and the support structure within acceptable levels up to 16 T.

The aluminum IC-clamps help the vertically split iron yoke retain a closed gap at operating temperature up to 17 T, providing a very rigid structure around the coils. The weld shrinkage of the stainless steel shell is achievable and the stresses remain at an acceptable level at all times. To counteract the very large electro-magnetic forces and to minimize the deformation of the coil, an optimized shim plan has been computed and presented.

The sensitivity analysis shows that the tolerances used in the study, cover a large design space which is reflected at the range of the resulting maximum equivalent stress in the coil. At the magnet nominal operation field of 15 T, the equivalent stress in the coil remains below 200 MPa for almost all parameter variations, which is a sign that there is margin in the design. The material properties of the coil have the largest impact on the maximum coil stress level, underlining the need for an in-depth examination of the actual material properties of the coil. The range of the shim thicknesses presented in this study account also for counterbalancing any geometrical imperfections may occur at any part, due to manufacturing instabilities.

REFERENCES

- [1] The U.S. Magnet Development Program Plan, <https://science.energy.gov>
- [2] A.V. Zlobin et. al., "Design concept and parameters of a 15 T Nb₃Sn dipole demonstrator for a 100 TEV Hadron Collider", Proc. of IPAC2015, Richmond, VA, USA, p.3365.
- [3] V. V. Kashikhin et al., "Magnetic and structural design of a 15 T Nb₃Sn accelerator dipole model", IOP Conference Series: Materials Science and Engineering, v.101, issue 1, p.012055, 2015.
- [4] I. Novitski and A.V. Zlobin, "Development and comparison of mechanical structures for FNAL 15 T Nb₃Sn dipole demonstrator", Proc. of NAPAC2016, Chicago, IL, USA, p.137.

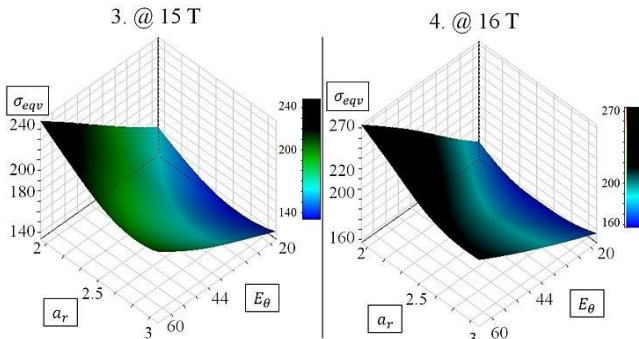


Fig. 9. 3D response surface of the maximum equivalent stress (MPa) in the coil, in correlation with the radial coefficient of thermal expansion $a_{r,coil}$ (mm/m) and the azimuthal module of elasticity $E_{\theta,coil}$ (GPa). The available design space at 15 T (in color), in which the equivalent stress at the coil is below the set goal of 200 MPa, is larger than the corresponding at 16 T. The region in black color presents combinations of parameters which do not fulfill the stress design goals.

- [5] I. Novitski et al., "Development of a 15 T Nb₃Sn accelerator dipole demonstrator at Fermilab", IEEE Trans. on Appl. Supercond., Vol. 26, Issue 3, June 2016, 4003006.
- [6] M. Karppinen et al., "Design of 11 T Twin-Aperture Nb₃Sn Dipole Demonstrator Magnet for LHC Upgrades", IEEE Trans. on Appl. Supercond., Vol. 22, Issue 3, June 2012, 4901504
- [7] C. Kokkinos et al., "The Short Model Coil (SMC) Nb₃Sn Program: FE Analysis with 3D Modeling", IEEE Trans. Appl. Supercond., Vol. 22, No. 3, June 2012.
- [8] PITHIA BEM software package, www.feacomp.com/pithia
- [9] T. Gortsas et al., "An advanced ACA/BEM for solving 2D large-scale problems with multiconnected domains", CMES: Computer Modeling in Engineering & Sciences, 107(4), pp. 321-343, 2015.